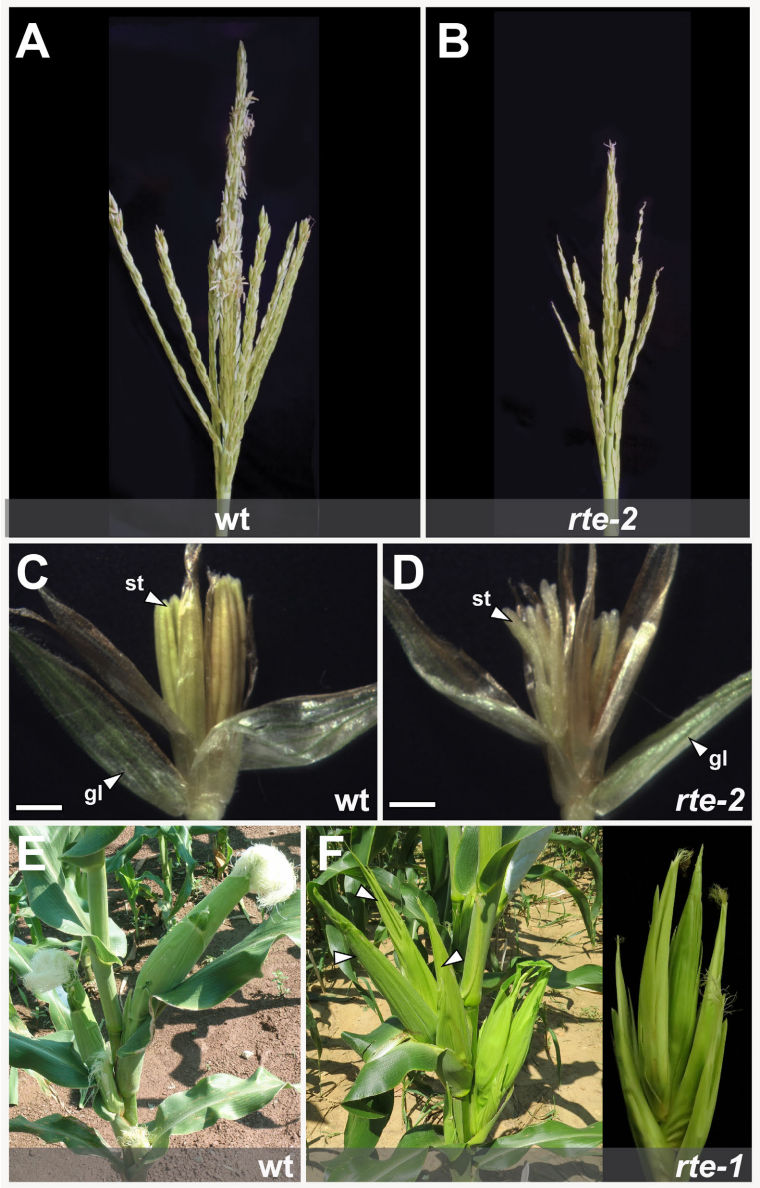

Supplemental Figure 1. Additional Phenotypes of *rte-1* and *rte-2* Mutants.
(A) Tassel of wild-type sibling and **(B)** *rte-2* mutant.
(C) and **(D)** Wild-type and *rte-2* spikelets showing two florets with stamens. Gl: glume; st: stamens.
(E) and **(F)** Wild-type ears are borne at the tip of a primary lateral branch **(E)**. In *rte* mutants, several ears (arrowheads) are borne on the primary lateral branch, due to activation of secondary axillary buds **(F)**.

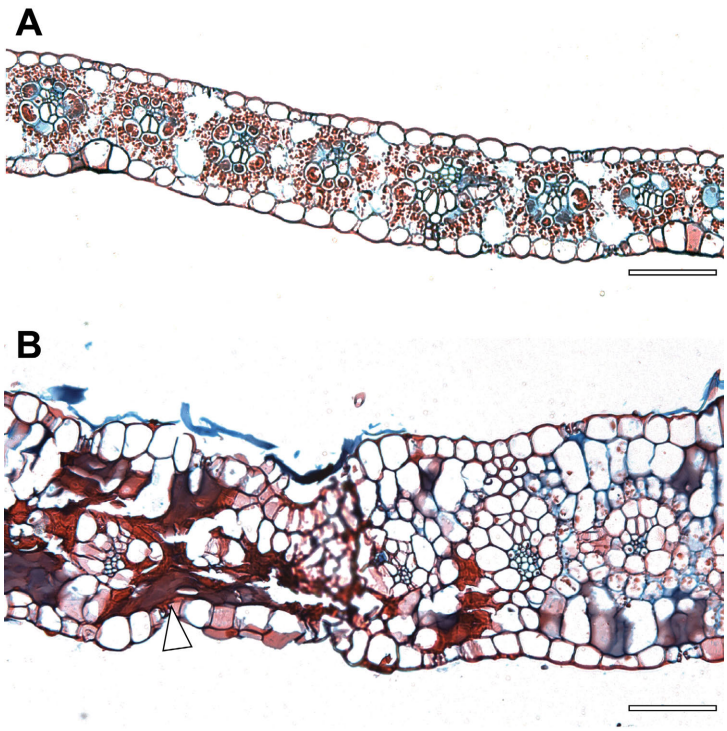

Supplemental Figure 2. *rte* Leaf Sections.
(A) and **(B)** Cross sections of leaves stained with Saffranin O/Alcian Blue. Lignified red patches (arrowhead) are observed in *rte* mutant leaves. Scale bars: 100µm

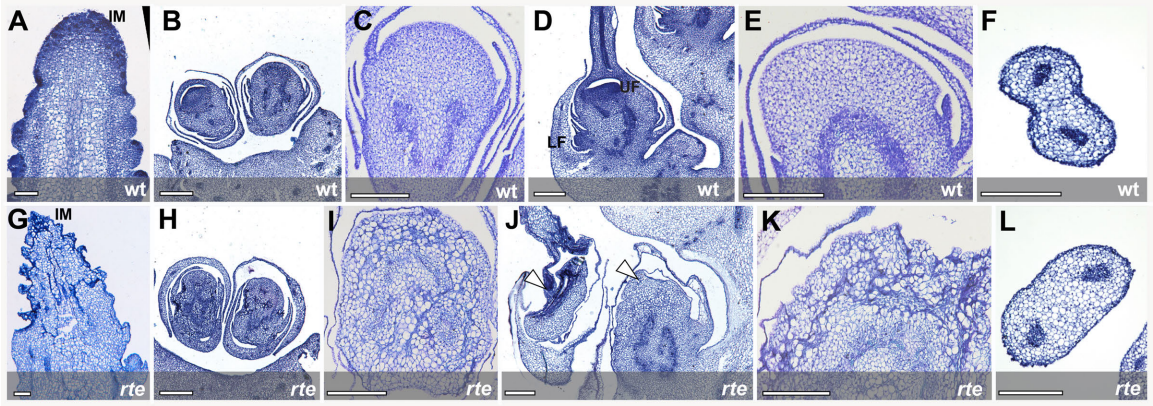

Supplemental Figure 3. Histological Analysis of *rte* Reproductive Development.
(A) and **(E)** Sections of ear tips in wild-type and *rte* mutants stained with Toluidine blue, showing the collapse of the inflorescence meristem (IM) and axillary meristems in *rte*. Scale bars: 100 µm.
(B-F) and **(G-L)** Sections of developing spikelets and florets from wild-type and *rte-1* stained with Toluidine blue. **(B,C)** and **(F,I)** Cross sections of paired spikelets. The sections are taken from the middle of developing spikelets. Note that in **(H)** the spikelets have begun to shrink at the margins, and in **(I)** the internal tissue organization is disrupted when compared to wild type **(C)**. **(D,E)** and **(J,K)** Longitudinal sections of developing florets **(D,J)** and floral meristems **(E,K)**. In the *rte* mutant **(J)** the meristems and developing floral organs have collapsed (arrowheads) and the tip of the meristems is wrinkly and its structure disrupted **(K)**. UF: upper floret; LF: lower floret. **(F)** and **(L)** Cross sections of silks from wild-type and *rte* appear morphologically similar. Scale bars: 200µm.

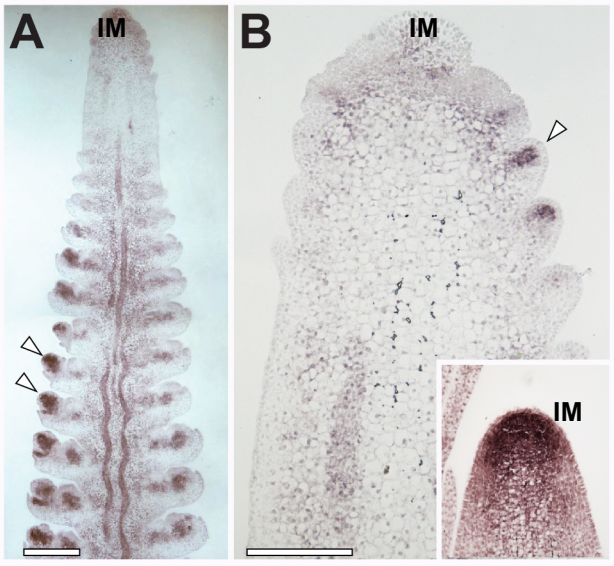

Supplemental Figure 4. In Situ Hybridizations of *rte-1* Ears Probed With the Meristem Marker *knotted1* (*kn1*).
(A) Immature ears showing *kn1* expression in spikelet meristems (arrowheads) and vasculature.
(B) Close-up view of a mutant *rte-1* inflorescence meristem. Strong *kn1* expression is only observed in SPMs (arrowhead) of the mutant but not in the inflorescence meristem where *kn1* expression is normally strong. The IM in this ear sample (~1cm stage) has already started to collapse. Inset: *kn1* in wild type inflorescence meristem (IM). Scale bars 200μm.

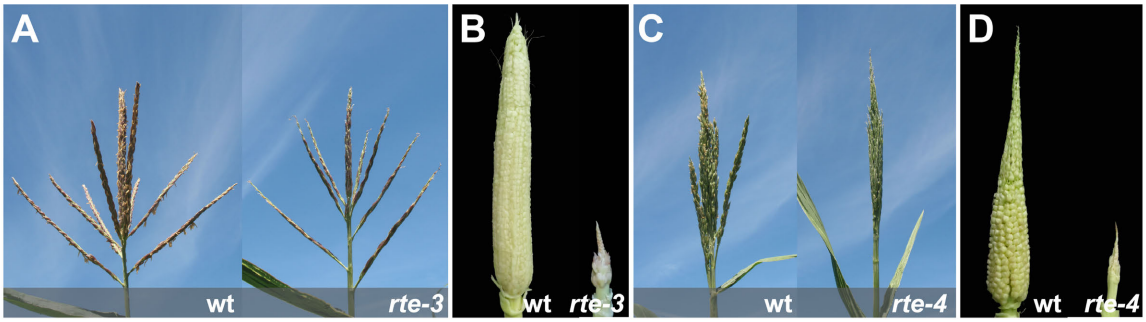

Supplemental Figure 5. The Tassel and Ear Phenotype of *rte-3* and *rte-4.*
(A) Wild type (left) and *rte-3* (right) tassels in an A632 background.
(B) Corresponding wild-type (left) and *rte-3* (right) unfertilized ears.
(C) Wild type (left) and *rte-4* (right) tassels in an A619 *ramosa2-R* background.
(D) Corresponding wild-type (left) and *rte-4* (right) unfertilized ears.

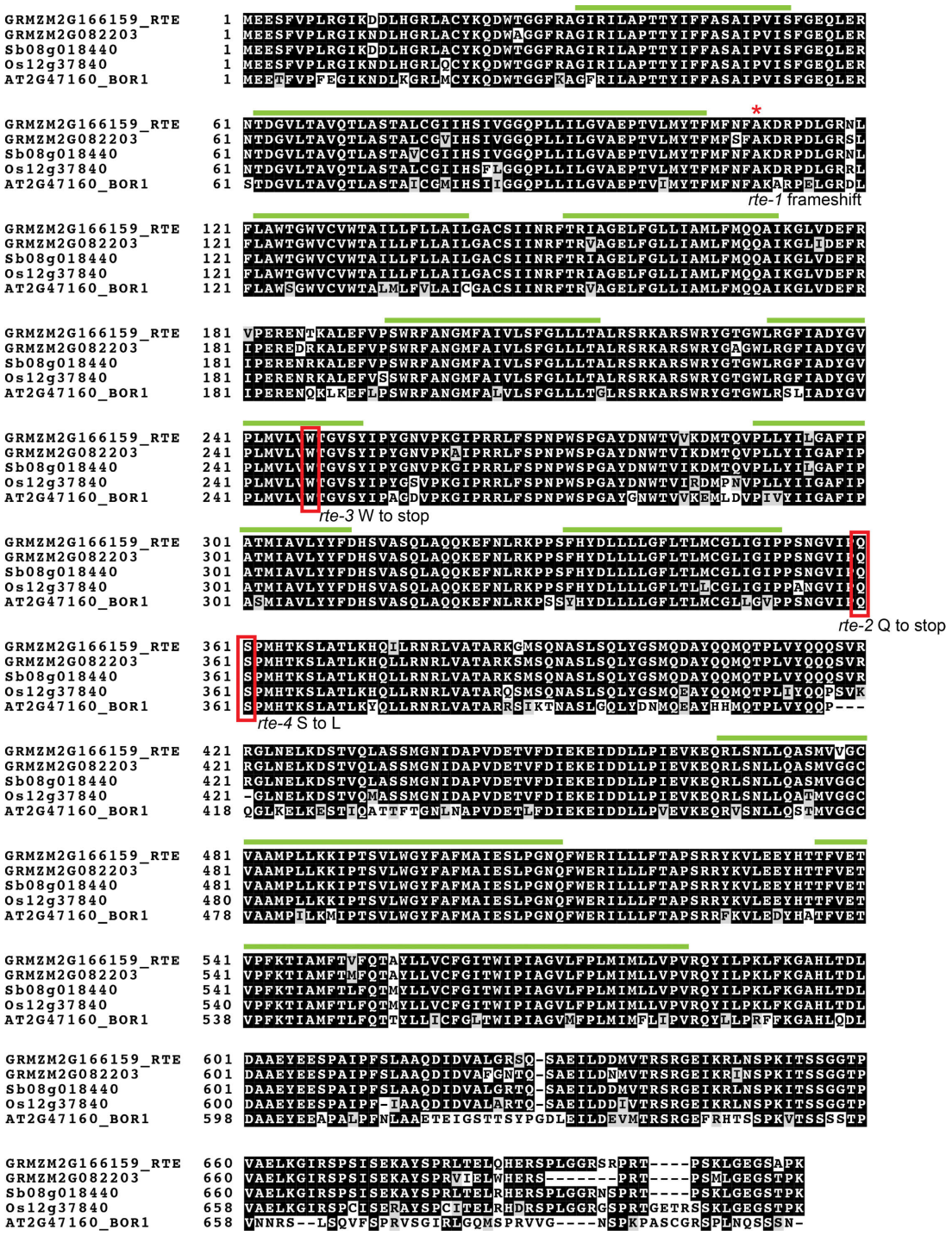

Supplemental Figure 6. Protein sequence alignment of BOR1 homologs in different species. The lesions of all four *rte* alleles are indicated in red. In green are marked the putative transmembrane domains. Sb, *Sorghum*; Os, *Oryza*; AT, *Arabidopsis thaliana*.

Supplemental Figure 7. Rescue of the *rte-1* Tassel Phenotype.
(A) to **(D)** Six representative *rte-1* tassels from plants grown at different concentration of boric acid: **(A)** 0μM; **(B)** 20μM; **(C)** 100μM; **(D)** 200μM.
A wild type tassel grown under same conditions is shown in the far right panel.

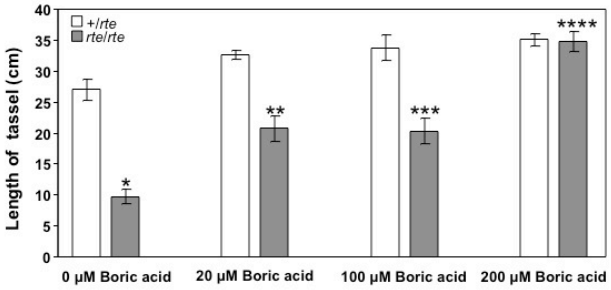

*ttest, P=0.00001168; **ttest, P=0.0002171; ***ttest, P= 0.001377, ****ttest, P= 0.8905144

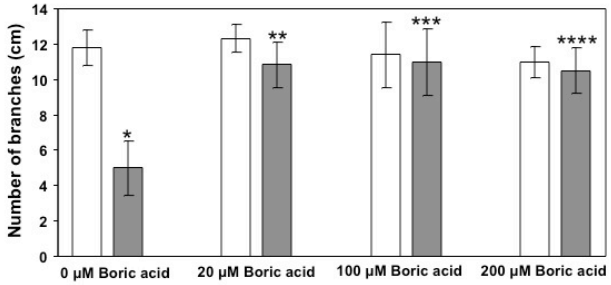

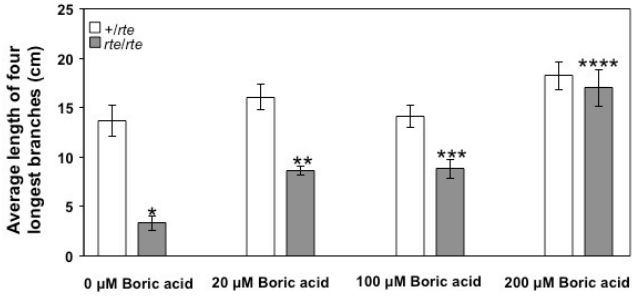

*ttest, P=0.000134; **ttest, P=0.000222; ***ttest, P= 0.006231;****ttest, P=0.578323

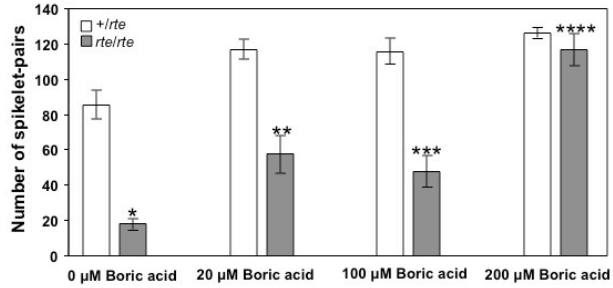

test, P= 2.17851E-06; **ttest, P=0.0004116; ***ttest, P= 0.00021280; ****ttest, P=0.283702175

Supplemental Figure 8. Rescue of the *rte-1* Tassel Phenotype. Quantification of tassel length, number of primary branches, length of primary branches and number of spikelet-pairs. Error bars, standard error.

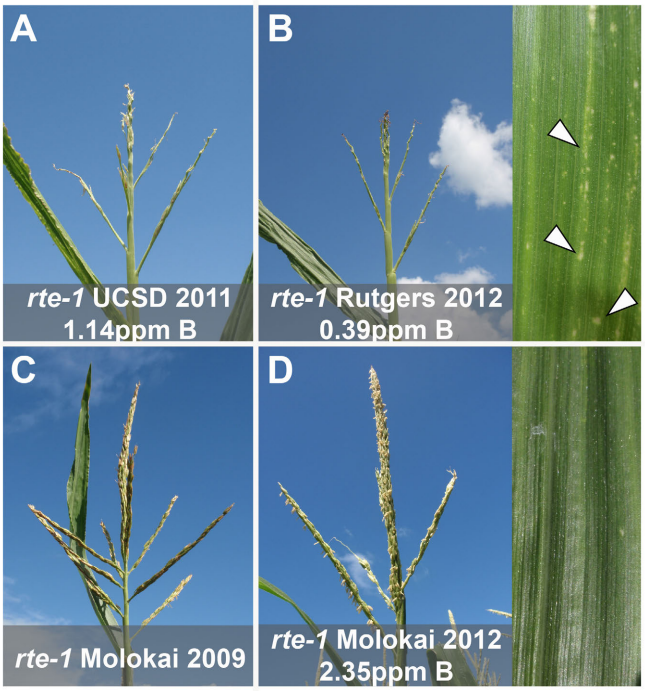

Supplemental Figure 9. The *rte* Phenotype is Influenced by the Boron Concentration in the Soil.
(A) to **(D)** Effects of different soil boron concentrations on the *rte* tassel phenotype. Representative tassels and leaves from *rte-1* mutant plants grown at three different locations where soil boron concentrations ranged from low (**B**; 0.39ppm) to moderate (**A**; 1.14ppm), and high (**D**; 2.35ppm). The comparatively boron-rich soil of Molokai consistently resulted in a relatively less severe phenotype **(C, D)**. In **(B)** and **(D)** a close-up of a leaf is provided. Note the lesions apparent in **(B)** (arrowheads) that are not present in **(D)**.

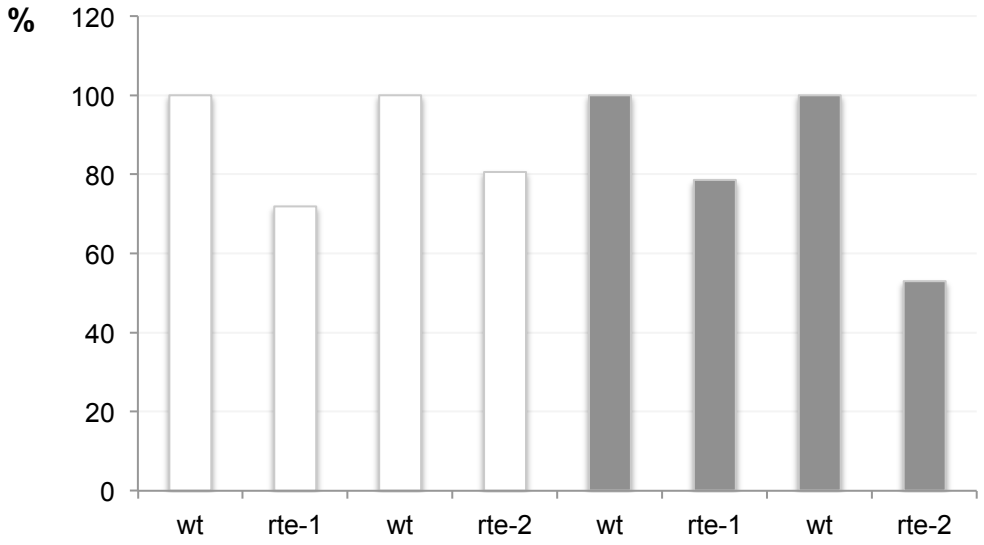

Supplemental Figure 10. Boron Measurements in *rte* Mutants.
Boron measurements expressed as percentage (Y axis) relative to wild type in leaf (white) and immature ear (grey) samples. Each sample is bulked tissue from at least three different plants.

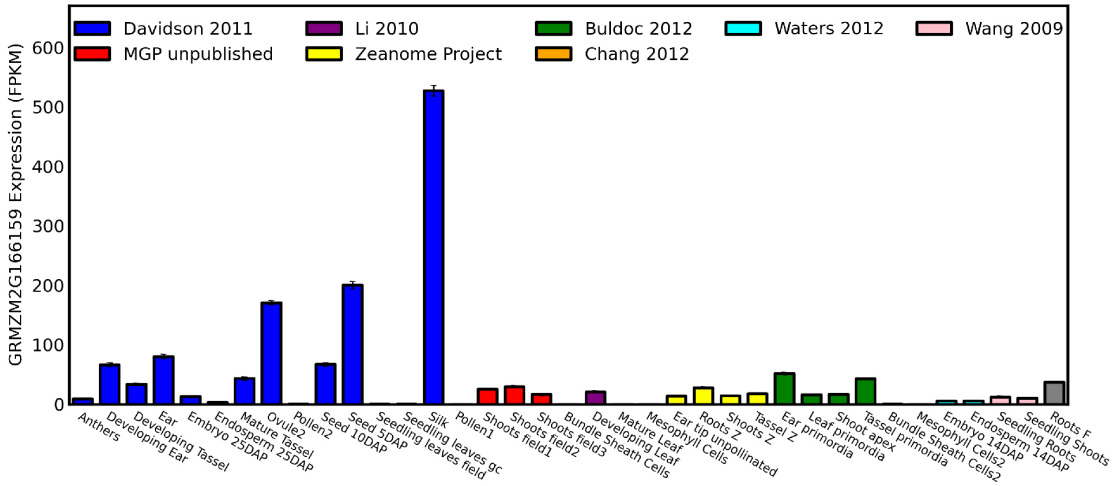

Supplemental Figure 11. Tissue-specific expression data of *rte* derived from multiple RNAseq datasets, available at www.qteller.com. Error bars represent the upper and lower FPKM limits.

Supplemental Table 1
List of primers used.

	PRIMERS 5'-3'	PURPOSE
MAGIv4_1364	For: GTTGACATCTCTACTACTAAGGTC Rev: AGCCTGGAGAAGATATGGACGACT	Indel marker
MAGIv4_55889	For: AGCAGCCTGCCTTATCTTCACAGC Rev: CTGATGTCAGGCTTGCAGCTACAC	dCAPS marker-digest with AluI
RTE-F1 RTE-R1	CCGACTGGCCATCCAGAATATACC GCACATGCCTTTGAGCAACCTACT	*rte* gene
RTE-F2 RTE-R2	CTCTGTGGCCATCTGGATGTGCGA TGCCATGTGAGTGAGAAATCAGATG	*rte* gene
RTE-F3 RTE-R3	CATCTGATTTCTCACTCACATGGCA GGAGTGCTATACCTGTAATCTCTG	*rte* gene
RTE-cds-F1 RTE-cds-R3	ATGGAGGAGAGCTTCGTGCCCTTG CACCATCGAAGCCTGTAGAAGGTTG	*rte* cds
RTE-cds-F3 RTE-cds-R2	ACAGGCTTCGATGGTGGTGGGCTGT TCACTTTGGTGCCGAGCCTTCACC	*rte* cds
rte-1	For: TACTTGTGCAGATGGAGTCCTCAC Rev: CTGCACGCAAACATGACAACAAC	CAPS marker-digest with StyI
rte-2	For: CCTCCATCAAATGGTGTCATTGTA Rev: GAAAATGTTATGTAAACAAATTGTCTG	dCAPS marker-digest with RsaI
BOR1-037312-F	ATGCTTGATGTTCCAATCGTC	*bor1* genotyping
BOR1-037312-R	ATCCATGTGAGACCAAAGCAG	*bor1* genotyping
LBb1.3	ATTTTGCCGATTTCGGAAC	*bor1* genotyping
RTE793-Nco-F	CGCCTTTTTAGCCCTAATCCATGG	RTE-L361 cloning
RTE1195-Leu-R	CGTATGCATGGGTAATTGTGGAATGACACCATTTGA	RTE-L361 cloning
RTE1069-Leu-F	GTCATTCCACAATTACCCATGCATACGAAGAGTTTG	RTE-L361 cloning
RTE2103-Stu-R	CTTGGATGGCGTCCTAGGCCTGCT	RTE-L361 cloning
RTE-pENTR-SFI-F	GAATTCGGCCGTCAAGGCCAATGGAGGAGAGCTTCGTGCCCT	*35S:RTE:YFP* transient assay
RTE-pENTR-SFI-R	AGTCGACGGCCCATGAGGCCCTTTGGTGCCGAGCCTTCACCC	*35S:RTE:YFP* transient assay
RTE-35s/pBJ36-XhoI-F1	GTCGACCTGCAGACGCGTCTCGAGATGGAGGAGAGCTTCGTGCC	*35S:RTE* complementation
RTE-35s/pBJ36-XhoI-R1	ACCCGGGGTACCGAATTCCTCGAGTCACTTTGGTGCCGAGCCTT	